

TEMPERATURE-CONTROLLED SELECTIVE LASER SINTERING

J. A. Benda

United Technologies Research Center
East Hartford, CT 06108

ABSTRACT

A control scheme for laser sintering has been developed which maintains sintering powder at constant temperature by actively controlling laser power. It uses a sensor to monitor the temperature of powder at the focus of a moving laser beam. The control scheme corrects for variations of thermal conductivity and powder reflectivity due to the proximity of previously sintered material, as well as for statistical fluctuations. The sensor also serves as a useful diagnostic, and is used to confirm model predictions of the variation of powder temperature with process parameters. A second temperature-controlled laser beam, concentric with the first, but of larger spot size, can be used to locally heat the powder around the sintering powder. This is shown to reduce curling as well as the balling or agglomeration of molten material.

INTRODUCTION

With the advent of stereolithography in 1988, a number of rapid prototyping technologies have been developed. The selective laser sintering process is potentially one of the most versatile [1]. An infrared laser selectively sinters layers of powder, producing a prototype part one layer at a time. Initially developed for wax and plastic materials, current research is directed towards extending the technology to sintering metal and ceramic materials directly [2].

Two problems have been inherent to the SLS process which limits its usefulness. One problem is that the thermal conductivity and reflectivity of powder changes as it is sintered, so that the amount of laser power required to uniformly sinter powder changes depending on the amount and proximity of previously sintered material. Furthermore, heat builds up in the powder bed as material is sintered so that the temperature change and thus the laser power required to sinter is less. Part growth near edges and poor adhesion between layers are possible detrimental effects. One approach to solving the problem is to keep track of the history of the part as it is sintered and passively change the laser power as the part buildup progresses, assuming one knows how to do this. For a complex part, this can be quite complicated.

A second problem is that thermal gradients created during the sintering process cause parts to curl. Previous attempts to control the curling problem have concentrated on heating the entire bed of powder up to some temperature less than that at which it starts to sinter during the time needed to build a part. The approach has been used with success for polymeric powders. For metal and ceramic parts, the approach is much more challenging because of the temperatures involved. Obtaining a uniform temperature distribution for the bed has proven difficult. Also, such powders will begin to sinter on their own at roughly half the melting temperature. Thus, it is not clear there is an operating window in which curling is controlled, but yet the powder bed does not cake up.

To solve the laser control problem, we have developed an active control scheme to keep the

temperature of the powder being sintered at the beam focus constant. A two beam approach to controlling curling was also explored, in which a large beam is used to locally heat the powder around a tightly focused beam which does the actual sintering. Because the heating time is short compared with the build time, it should be possible to achieve more local heating without the powder bed caking than is possible with the approach described above.

ACTIVE CONTROL SCHEME

The key element for the control scheme is a temperature sensor which can monitor the temperature of powder at the focus of a moving laser beam. The sensor is schematically illustrated in Figure 1. A dichroic beamsplitter or a scraper mirror is inserted into the beam path before the scanning mirrors. This optic element allows the infrared laser beam to pass through unattenuated, but reflect thermal emission from the powder in the wavelength range of a detector. In our experiment, a CO₂ laser is used lasing at 10.6 μm, and a germanium detector is used which is sensitive to wavelengths from 1.0 to 1.8 μm. A lens is used to image the powder bed onto the detector. If desired an aperture can be put in front of the detector to insure that only thermal emission at the laser beam focal spot is monitored. Another aperture should be in the system to insure that the solid angle of the thermal radiation reaching the detector does not change as the scanning mirrors are rotated. By putting the sensor before the scanning mirrors, the detector will automatically follow the moving beam.

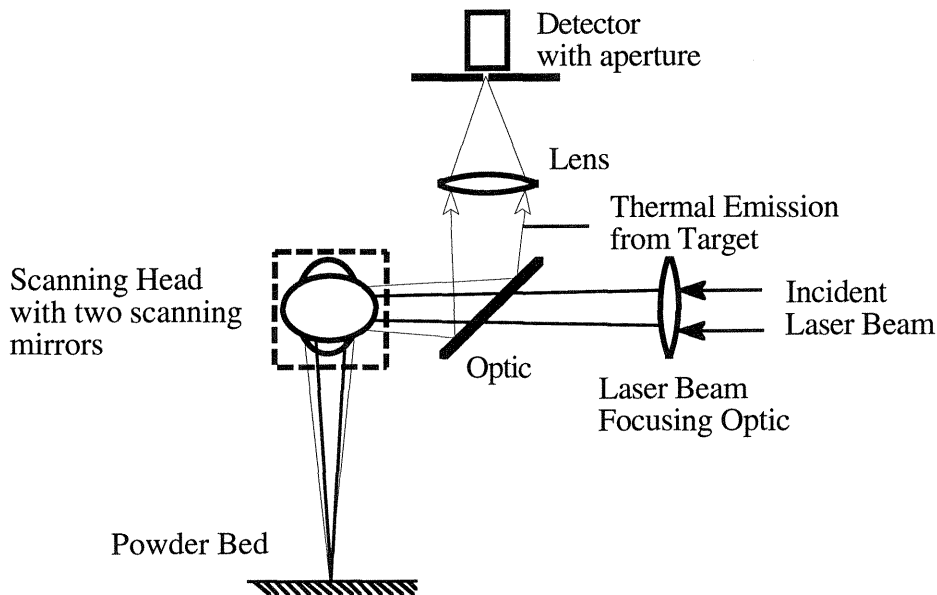


Figure 1. Schematic of thermal sensor.

We have performed tests with a variety of materials and have concluded that primarily thermal emission is seen by our detector. There is no evidence of plasma or a plume being produced at the power levels necessary to sinter powder. The amount of radiation we are seeing as well as the wavelength dependence are consistent with thermal emission. The wavelength dependence of the emission from two ceramic powders was measured with a scanning monochromator and a photomultiplier. The wavelength dependence of the photomultiplier sensitivity, as well as the

grating efficiency of the monochromator, can be normalized out by dividing the signal produced by sintering ceramic materials with that produced by a quartz-tungsten-halogen (QTH) lamp. A QTH lamp approximates a black body source at 3200 °K. The resulting curves were fit assuming thermal emission to derive the temperatures of the ceramic materials, as shown in Figure 2. The temperatures are within a couple of hundred degrees of the melting or sublimation temperatures of these materials as was expected, since some melting or vaporization of material was observed. Although only a few points are plotted, the emission was measured continuously and no structure indicative of anything other than thermal emission was observed.

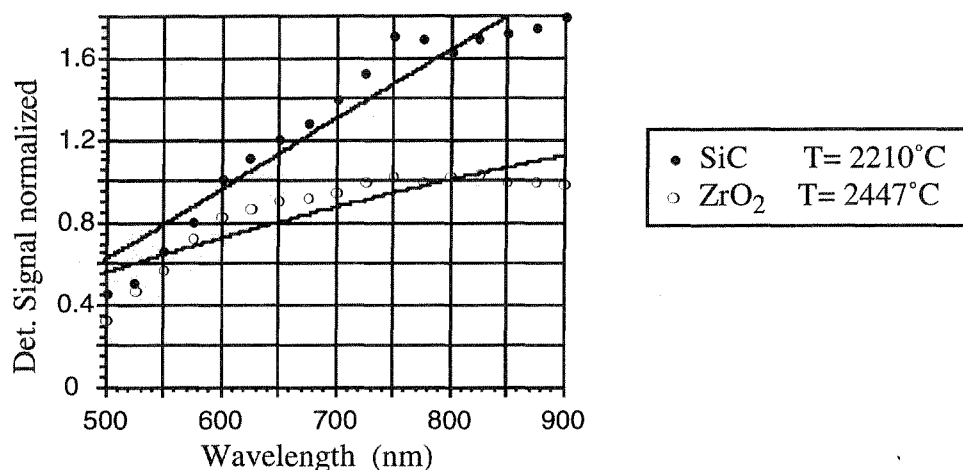


Figure 2. Color Temperature determined by normalizing emission to QTH Lamp.

As a second test, our detector was calibrated and the total irradiance on it agreed with a calculation of thermal emission using the numerical aperture of our collection optics and assuming a reasonable value of emissivity. This test was done with iron powder and just enough laser power to start melting the iron - implying a temperature of about 1500 °C.

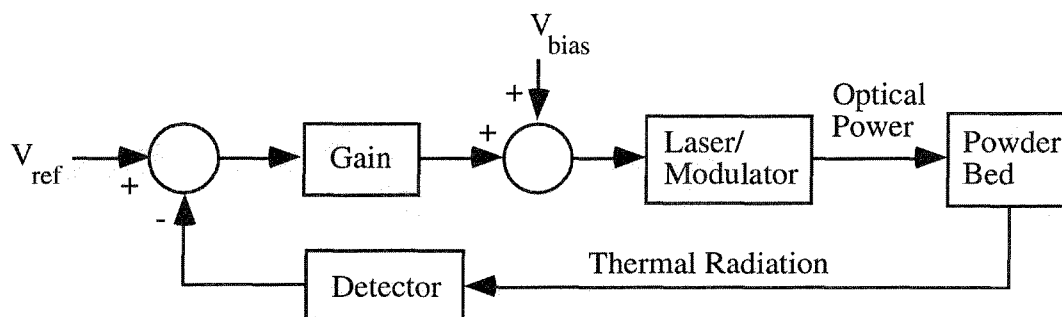


Figure 3. Block Diagram of Control Scheme

The signal from the germanium detector was used to control laser power. Initially this was done with an acousto-optic modulator external to the laser. The modulator uses acoustic waves at rf frequencies to produce a phase grating in a germanium crystal. This grating deflects a portion of the laser beam. Modulating the rf power modulates the beam transmitted directly through the crystal. The laser beam passes first through the modulator, then through a 10X telescope which expands the beam, a concave mirror to focus the beam, and finally two scanning mirrors which

direct the focused beam to the powder. The focused spot size was about 0.3 mm. An analog driver for the AO modulator was used which allowed the laser power to be varied continuously between 10 and 100 per cent of full power. The modulator was initially biased to give about 50% power. A block diagram of our control loop is shown in Figure 3. The control circuit used generated an error signal between the actual detector signal and the desired signal, multiplied it by a variable gain, and used the resulting signal to drive the AO modulator.

A mixture of tungsten and copper powder was used to evaluate the performance of our system. Three adjacent, slightly overlapping scans were made across the initially unsintered powder bed. Figures 4 gives oscilloscope traces comparing the open loop and closed loop performance. The top trace in both plots shows the laser power, which goes to zero between the three successive scans, while the bottom trace shows the germanium detector signal. For open loop operation, the laser power remains constant, but the detector signal is much higher on the first scan and is noisy. For closed loop operation, the detector signal is now constant and the laser power varies, increasing after the first scan by roughly 20%.

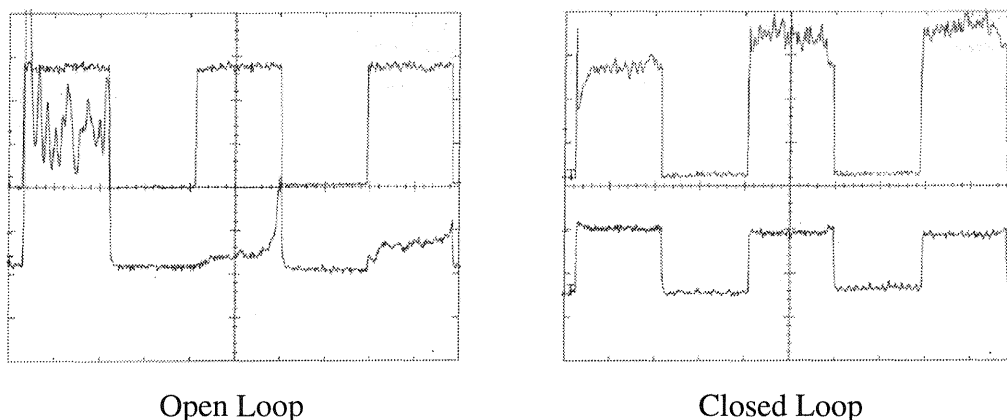


Figure 4. Comparison of open loop and closed loop performance of control scheme with W/Cu mixture. The upper oscilloscope traces are laser power. The lower traces are Ge detector signal. The results from three adjacent scans of the powder are shown.

Examination of the irradiated powder shows that the first open loop scan digs a trench in the powder with molten copper sinking well into the tungsten powder (the power coupled in was too great), while successive scans do not adequately couple into the powder. Under closed loop control, the irradiated powder is uniformly sintered. Examination of the microstructure also reveals that molten copper is more uniformly distributed even within one scan line. This may prove to be as big a benefit for closed loop control as compensating for the previous history of the sintered part. A significant decrease in sensor signal is always noted from the first to the second scan with no feedback control, with the effect more pronounced for the tungsten/copper mixture than for most materials tried.

Recently, we have acquired a 200 W rf-excited laser (SYNRAD model 57-2) and confirmed that it is possible to modulate the laser power directly through pulse width modulation of the rf power supply with performance comparable to that with the AO modulator without its power

limitations. Modulation up to 5 KHz appears possible. Figure 5 shows results on mullite powder (aluminum silicate). The ability to correct for temperature variations is dramatic.

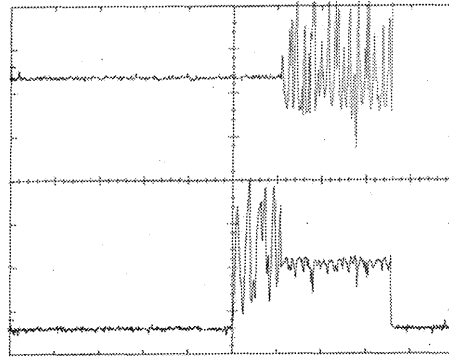


Figure 5. Comparison of open loop and closed loop performance with mullite powder using pulse width modulation. The upper oscilloscope trace is the voltage used to modulate laser power. The lower trace is the Ge detector signal. Closed loop control is turned on part way through a single scan on unsintered powder.

The detector signal is a particularly strong discriminant, varying rapidly with both laser power and scan speed. Measurements of the detector signal as a function of the scan velocity at several laser powers are shown in Figure 6 (using Argon as a cover gas) for sponge iron powder from Pyron Corp. At a detector signal of 15 mv, some of the iron powder is just beginning to melt. So it is reasonable to assume that the powder was near the melting temperature of 1500°C. Using that, it is possible to calculate the temperature rise per watt of laser power for each scan speed.

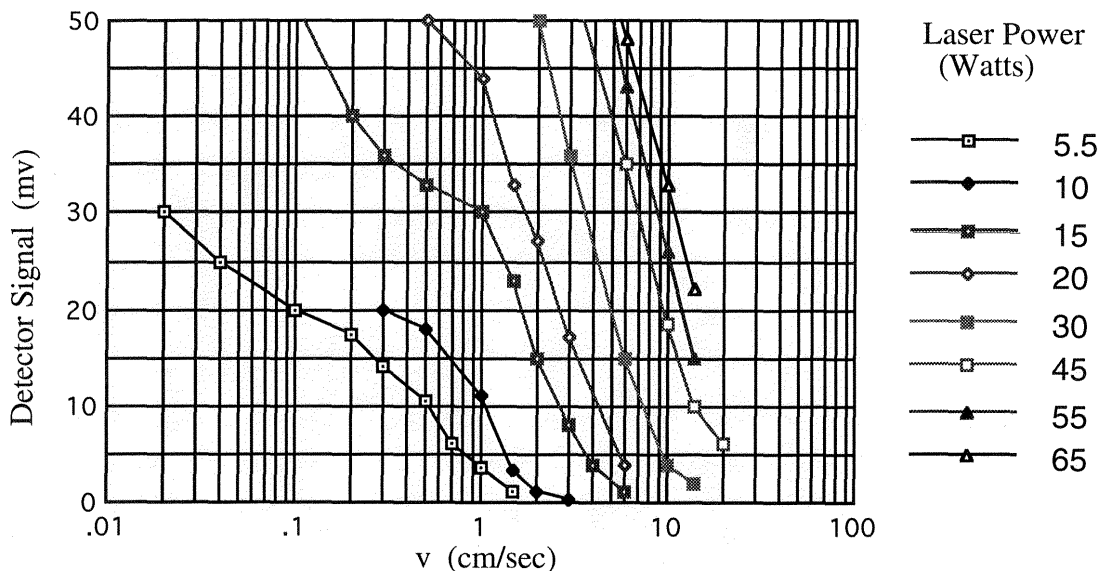


Figure 6. Detector signal versus scan speed for several laser powers.

It is possible to predict the peak temperature rise per watt for a moving Gaussian laser beam fairly simply, if one assumes a constant thermal conductivity. The temperature rise at a given position is given by (derived in a manner similar to results in [3]),

$$\Delta T = \frac{2\varepsilon_s P}{\pi w^2 \rho C_p} \int_0^\infty \frac{w^2/2}{w^2/2 + 4\alpha^2 t'} \exp\left(-\frac{(x+vt')^2 + y^2}{w^2/2 + 4\alpha^2 t'}\right) Z(t', z) dt' \quad (1)$$

where

$$Z(z, t') = \frac{\beta}{2} \left\{ \operatorname{erfc}\left(\beta\alpha\sqrt{t'} - \frac{z}{2\beta\alpha\sqrt{t'}}\right) \operatorname{sgn}\left(\beta\sqrt{t'} - \frac{z}{2\beta\alpha^2\sqrt{t'}}\right) e^{-\beta z} + \operatorname{erfc}\left(\beta\alpha\sqrt{t'} + \frac{z}{2\beta\alpha\sqrt{t'}}\right) \operatorname{sgn}\left(\beta\sqrt{t'} + \frac{z}{2\beta\alpha^2\sqrt{t'}}\right) e^{+\beta z} \right\} e^{\beta^2\alpha^2 t'} + \beta e^{-\beta z} e^{\beta^2\alpha^2 t'} \theta\left(\frac{z}{2\alpha^2 t'} - \beta\right)$$

Here ΔT is the temperature rise, P is the laser power, ε_s is the emissivity of the powder surface, α^2 is the thermal diffusivity ($k/\rho C_p$), ρ is density, C_p is heat capacity, w is the Gaussian spot size, β is the penetration depth of the radiation into the powder assumed to be exponentially decaying, v is the scan velocity taken to be in the x direction, y is the transverse coordinate on the powder surface, z is the depth into the powder, $\operatorname{sgn}()$ is unity with the sign of the argument, and

$$\theta(x) = \begin{cases} 1 & x \geq 0 \\ 0 & x < 0 \end{cases}$$

All coordinates are with respect to the beam center on the surface.

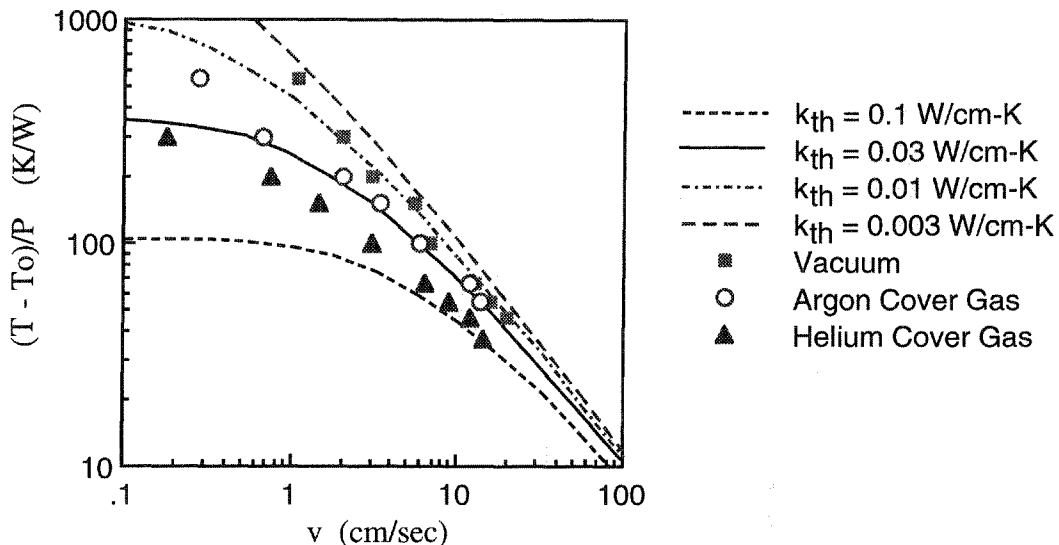


Figure 7. Temperature rise per watt of laser power. Experiment and theory.

The calculated peak temperature rise per watt of laser power is plotted versus scan velocity in Figure 7 for a range of thermal conductivities. Also plotted are experimental curves for iron powder with two different cover gases, helium and argon, and under vacuum. The cover gas modifies the thermal conductivity of the powder with roughly an order of magnitude change predicted in going from vacuum to helium, argon being intermediate [4]. At low scan speeds, thermal equilibrium is established and the temperature rise is independent of speed and varies inversely with thermal conductivity. At high speeds, the power stays where it is deposited during the dwell time of the beam at a given position. Thus the temperature rise varies inversely with scan speed and is independent of thermal conductivity. This behavior is nicely mirrored in the

experimental data, giving some confirmation of the assumption that the radiated power is mainly thermal emission, as well as some confirmation of the theory.

TWO BEAM SINTERING

We first implemented two beam sintering by using the deflected beam from the AO modulator used for feedback control, as shown in Figure 8. The deflected beam was diverted around the 10X telescope and sent directly to the focusing optic. (In the single beam experiments above this beam was blocked.) Because that beam was ten times smaller, its focused spot size is about ten times larger. (The focused spot size varies as $2\lambda f/D$, where f is the focal length, λ is wavelength and D is the initial beam diameter.) The two beams were nominally concentric at focus, although there may be reasons for having one beam lead the other. The modulator was biased so that roughly 80% of the power was in the deflected beam. One drawback of the approach is that if the AO modulator is used for control of the focused beam, any power which is removed from the focused beam is dumped in the defocused beam. But normally the defocused beam is much larger in power, so the percentage change is small.

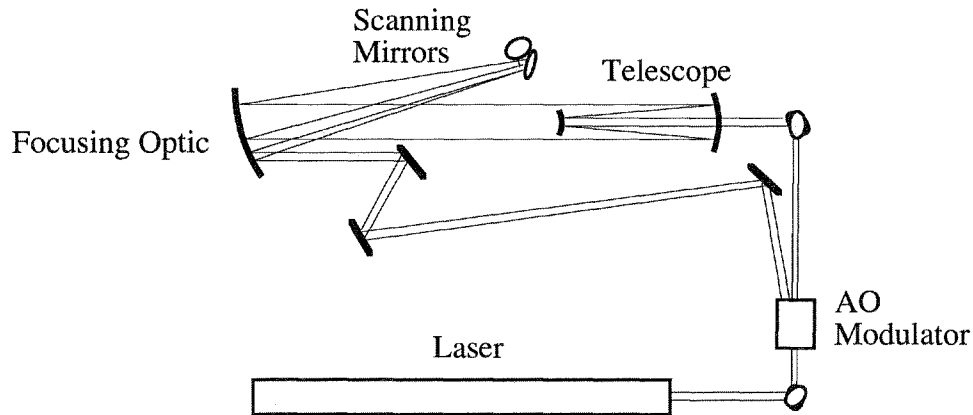


Figure 8. Schematic of two beam sintering experiment.

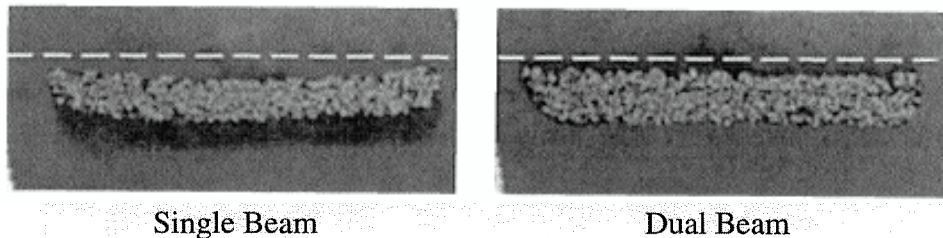


Figure 9. Comparison of curling for two sintered layers of iron/bronze powder using a single laser beam and a dual beam. Sintered material is shown in cross-section perpendicular to scanning direction. Dashed line is for visual reference.

Figure 9 shows the cross section of two layers of an iron/bronze powder mix, sintered with and without the larger beam. The samples were potted in epoxy and ground down to expose the cross section. The powers were adjusted to give the same signal in our germanium detector, so the

actual sintering temperatures used should be close. It is clear that much less curling results with two beam sintering. Without optimization, curling is not always eliminated, but is always observed to be reduced.

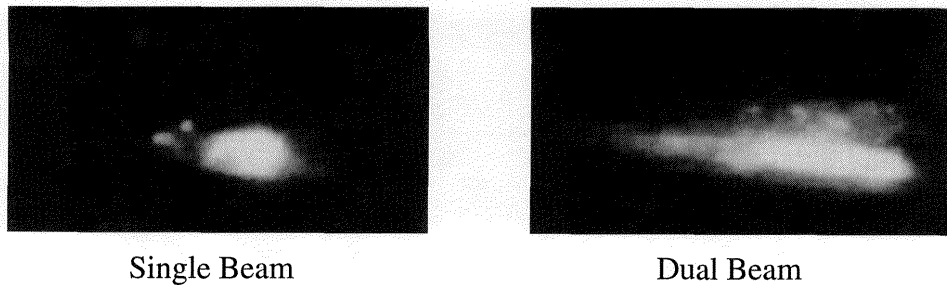


Figure 10. Images of selective laser sintering of alumina powder.

As is expected, the sintered material cools more slowly with the second beam. This might be part of its advantage. Figure 10 shows high speed video images of alumina powder being sintered with and without the second beam. The longer tail, as well as the hot powder to the side of the sintered material is clearly evident.

CONCLUSION

Our CO₂ laser, a SYNRAD Duo-Lase™ Model 57-2, has two independent lasers in a single housing with separate controllers and power supplies. A polarization beamsplitter combines the two beams, which are of orthogonal polarization. Each laser can be used to provide one of the two beams for dual beam sintering. We have successfully demonstrated two beam sintering with active control of both beams. A polarization beamsplitter is used to separate the two beams. A separate feedback control circuit is used for each laser. The aperture in front of the detector of figure 1 is now a mirror which is used to reimage the thermal emission from the powder irradiated mainly by the large beam. The second detector is part of the control loop for the large laser beam. Preliminary results indicate that controlling the large laser beam may be more important than control of the focused laser beam. More uniform sintering has been demonstrated. Complete elimination of the curling problem using dual beam sintering alone appears unlikely, at this point, but hopefully the problem can be significantly reduced.

REFERENCES

1. Deckard, C. R., *Part Generation by Layerwise Selective Sintering*, Master's Thesis, The University of Texas at Austin, May 1986.
2. Das, S., McWilliams, J., Wu, B., and Beamon, J. J., *Design of a High Temperature Workstation for the Selective Laser Sintering Process*, Solid Freeform Fabrication Symposium, The University of Texas at Austin, Aug. 12-14, 1991.
3. Rosenthal, D., *The Theory of Moving Sources of Heat and Its Applications to Metal Treatments*, Transactions of the ASME (Nov. 1946).
4. Swift, D. L., *The Thermal Conductivity of Spherical Metal Powders Including the Effect of an Oxide Coating*, Int. J. Heat Mass Transfer **9**, 1061-1074 (1966).